Sri Lankan Journal of Physics, Vol. 15 (2014) 19-29

INSTITUTE OF PHYSICS – SRI LANKA

Research Article

Sodium nickel oxide nanoporous cathodes used for sodium-ion rechargeable batteries

R.C.L. De Silva[1*], M.T.V.P. Jayaweera[1,3], V.P.S. Perera[2], I.P.L. Jayarathna[1] and S.R.D. Rosa[3]

[1]*Materials Technology Section, Industrial Technology Institute, Colombo 07, Sri Lanka*

[2]*Department of Physics, The Open University of Sri Lanka, Nawala, Sri Lanka*

[3]*Department of Physics, University of Colombo, Colombo 03, Sri Lanka*

Abstract

The initial research on rechargeable batteries started focusing on both Lithium and Sodium but Lithium was more attracted because of its higher energy density. Later considering the cost of lithium, research has been directed to explore the possibility of using Sodium for rechargeable batteries because of its high abundance and low cost compared to Lithium.

In this study we focuses on sodium Nickel oxide as the cathode material of the sodium iron rechargeable battery and tests were carried out to find the formation of crystal structure. Synthesis of Na_xNiO_2 nonporous active material were made using solid state reactions at 700˚C and the material development was studied by XRD characterizing technique. The developed Na_xNiO_2 was used as the active cathode material in a rechargeable half cell. The characterization confirmed the crystal structure of $NaNiO_2$ to be monoclinic, and also its surface morphology. Electron transition status test revealed the specific energy band gap to be 5.16 eV. Charge transfer resistance of the cathode material obtained was 13,121 Ω.

The further investigations on charge discharge revealed the maximum efficient charging rate per gram as 7.5 mA for 0.12 hours and maximum rate of discharge for maximum charge retention as 25 mA rate of charge per gram of Na_xNiO_2 which was the active

* Corresponding Author Email: chinthakades@yahoo.com

material of the rechargeable cell. The charge discharge cyclability was tested for Sodium Nickel Oxide with 0.2 mA constant current for both charging and discharging. A voltage of 2.34 V was observed as the open voltage (no load) at the beginning and the half cell showed more than 180 charge-discharge cycles in performance including a rest time of one minute for each cycle. This confirmed that the battery is able to hold a fairly high reversibility.

Keywords: Na^+ ion; Rechargeable batteries; $NaNiO_2$

---

1. INTRODUCTION

Applications of Lithium-Iron rechargeable batteries range from smaller energy required applications, such as portable electronics, to powering of hybrid vehicles. Lithium is utilized in the rechargeable battery technology due to its high energy density and power capacity[2-6]. Initial research started at the period of 1970-1980s by focusing on both Lithium and Sodium, however, it was Lithium that was more attracted because of its higher energy density. Later considering the availability and costs factors, researchers have focused their attention to explore the possibility of Sodium usage for rechargeable batteries because of its high abundance and low cost compared with Lithium[1].

Sodium-ion battery research is relatively young compared with other battery technologies but has a greater potential due to high abundance and low cost of sodium. The mined basic raw material trona, i.e. $Na_3(CO_3)(HCO_3)\,2H_2O$, is about 30-40 times cheaper than lithium carbonate[7], and redox potential ($E^0_{(Na+/Na)}$=2.71 V versus standard hydrogen electrode), only 0.3 V above that of lithium.Therefore rechargeable electrochemical cells based on sodium also hold much promise for energy storage applications. Transition metal oxides with the layered structure and alternating layers of Na and M (M = 3d transition metal such as Ni, Co, Mn, Fe, Cu) residing in the oxygen octahedral interstices have been extensively studied for these cells.

Recently, Terasaki *et al*., (1997) discovered the outstanding thermoelectric properties of the layered sodium cobalt oxides $Na_{(1-x)}CoO_2$ (x = 0.5). Aydinol *et al*., (1997, 1998) have studied the intercalation properties of various lithium metal oxides, sulfides and selenides. Moreover, it has been investigated the effects of the structure, metal and electrochemistry. They have found that both electrochemistry and structure have an effect on the battery voltage, but contribution from electrochemistry is considerably higher. Therefore, they demonstrated that when more electron transfer to oxygen occurs, a higher lithium intercalation potential is obtained. Benco *et al*., (1992) studied the influence of both the structure and the transition metals on the bonding.

The present study focuses on sodium nickel oxide as the cathode material of the sodium iron rechargeable battery and tests have been carried out to find the formation of crystal structure. Further investigations on the charge/discharge revealed the maximum

efficient charging rate and the maximum rate of discharge for a maximum charge retention on a Na_xNiO_2 rechargeable cell.

2. EXPERIMENTAL

2.1 Synthesis of cathode material

For the preparation of $NaNiO_2$ samples Na_2CO_3 and $Ni(NO_3)_2$ were mixed and grinded in an agate mortar at stoichiometric ratios of 1:2. The sample carrying crucible was placed on top of a hotplate whose temperature was gradually raised to 200˚C in two hours to remove moisture. The fully dried samples were fired continuously at 700˚C for 24 hours inside a furnace. The samples were slowly cooled down to room temperature and grinded again to obtain the ash colored fine powder of $NaNiO_2$ which is the active cathode material for the sodium-ion batteries.

2.2 Fabrication of half cell

Synthesized material was used to fabricate cathodes of sodium ion batteries as active material (AM) on stainless steel plates by spreading a slurry made grinding $NaNiO_2$ 85% with 5% acetylene black (AB), and 10% polyvinylidene fluoride (PVdF), dissolved in 1-methyl-2-pyrrolidinone (NMP) as the binder (AM mass is 1 mg cm^{-2}) and leaving for slow drying. Construction of the battery was performed in a N_2 atmosphere using a sodium foil as the anode. Polyester membrane placed as the separator was soaked with the electrolyte consisting of a 1 M solution of $NaClO_4$ in propylene carbonate. Charge/discharge tests were performed to find the efficient full charge cycle and to determine the maximum charge retention and the discharge rate.

2.3 Electrical contacts

Electrical contacts were firmly made to touch the electrodes to avoid any voltage drop. Soldering material made as a bubble located on either jaws of each crocodile clips were used for this purpose.

2.4 Measurements

X-ray diffraction (XRD) characterization was performed on the resulting powder with Regaku ultima VI, X-ray Diffractometer using Cu K_α (λ= 1542 Å) radiation to analyze the structure of the sample. Crystallographic information was obtained with the aid of the ICDD data base. Scanning electron microscopic tests (LEO 1420 vp) were carried out to study the formation of cathode material with maximum enabled instrument resolution.

The Fourier Transformed Infrared spectroscopy (FTIR) (Bruker Tensor 27) was carried out to determine type of the atomic bonding in composites. UV-visible absorption spectroscopy (Shimatsu 120) was used to find the energy band gap of the developed composite.

Charging/discharging tests and cyclic voltammetric measurements were performed (Biologic 150) to find the charge retention of developed NaNiO half cells.

Impedance spectroscopic measurements were done on half cells to find the impedance of cathode material and to construct equivalent circuit matching with the impedance data.

3. RESULTS AND DISCUSSION

3.1 XRD ANALYSIS

The XRD tests were carried out to monitor the proper formation of the crystalline structure of the synthesized cathode material. XRD patterns of the $NaNiO_2$ sample is shown in Figure 1. The content of sodium effects the structure of the sodium nickel oxide and the monoclinic structure phase is observed in the final product which was confirmed with h,k,l values, d values and 2θ values related to peaks **[1]** 4,0,0 / d=4.90 / 2θ=18.07, **[2]** 2,1,-1/ d=3.20 / 2θ=27.83, **[3]** 3,1,0 / d=3.08 / 2θ=28.96**, [4]** 3,1,-2 / d=2.76 / 2θ=32.41, **[5]** 4,1,1 / d=2.64 / 2θ=33.83, **[6]** 6,1,-1 / d=2.41 / 2θ=37.21, **[7]** 6,0,-4 / d=2.55 / 2θ=39.94, **[8]** 8,0,2 / d=2.02 / 2θ=44.61, **[9]** 11,1,-4 / d= 1.48 /2θ=62.04**, [10]** 12,1,3 / d= 1.26 / 2θ=75.39, **[11]** 4,3,-5 / d= 1.01 / 2θ=99.35 by comparing them with the standards[12].

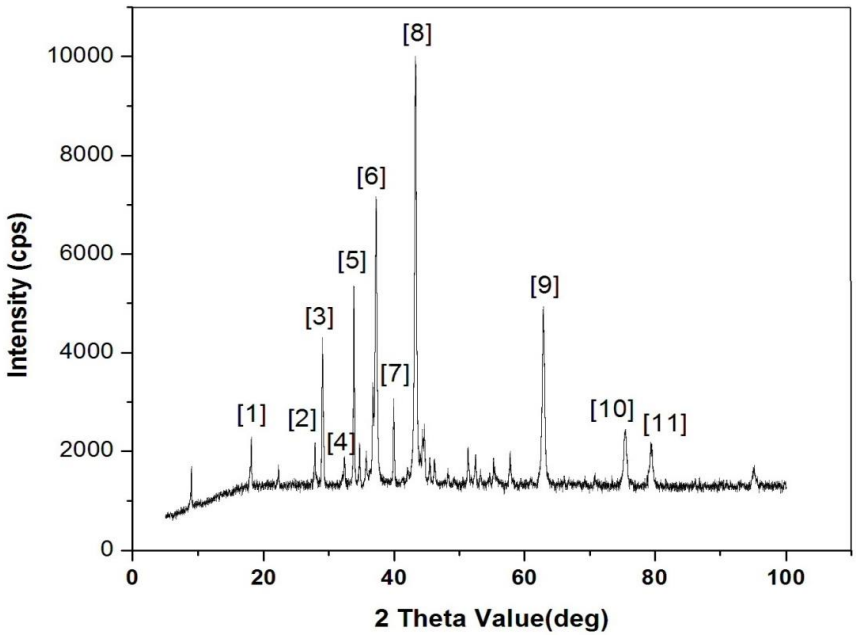

Figure 1: XRD pattern of $NaNiO_2$

3.2 SEM Analysis

To confirm the nanoporous nature of the $NaNiO_2$ cathode material the samples were examined with SEM using different magnifications. The crystals could be seen as clusters of smaller particles. A selected cluster was examined by higher magnification levels as seen in Figure 2. The micron level cavities were seen formed as when the cuboid shaped particles constructed with hexagonal unit cells, attached with each other. This enables the Na ions to intercalate in the cathode material.

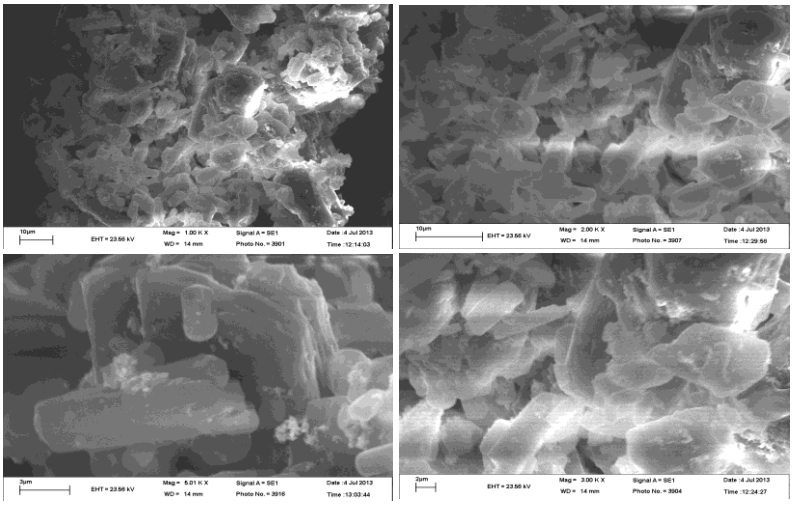

Figure 2: SEM images of $NaNiO_2$ composites

3.3 FTIR Analysis

The Fourier Transformed infrared spectra (FTIR) depicted in Figure 3 was used to analyze the bond formation of the cathode material. The bands appeared at the range of 847 cm^{-1} to 639 cm^{-1} refers to different types of asymmetric Ni-O bond vibrations.The metallic bonds that are expected at the region around 439 cm^{-1}cannot be studied by the FTIR technique. The peaks at 1057 cm^{-1}, 1174 cm^{-1}, 1353 cm^{-1} can be attributed to different types of bond vibrations on structural –OH groups.

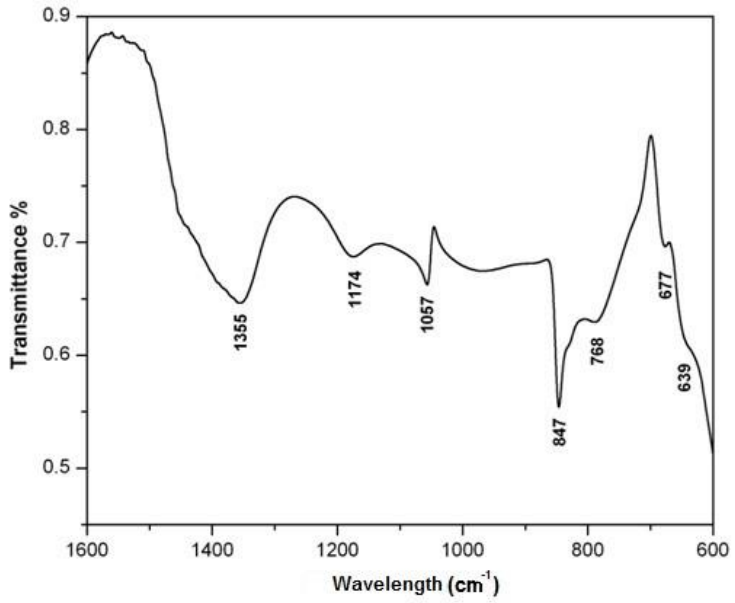

Figure 3: Fourier Transformed Infra-Red Spectrum of $NaNiO_2$ composite

3.4 UV-visible spectroscopic Analysis

According to the UV absorption spectra shown in Figure 4 the $NaNiO_2$, cathode material shows a dramatic increase of absorption beyond 240 nm. The use of equation of $E=hc/\lambda$ where E ,h, c and λ stands for energy, Plank constant, velocity of light and wave length respectively, revealed that the band gap of the composite material was about 5.16 eV.

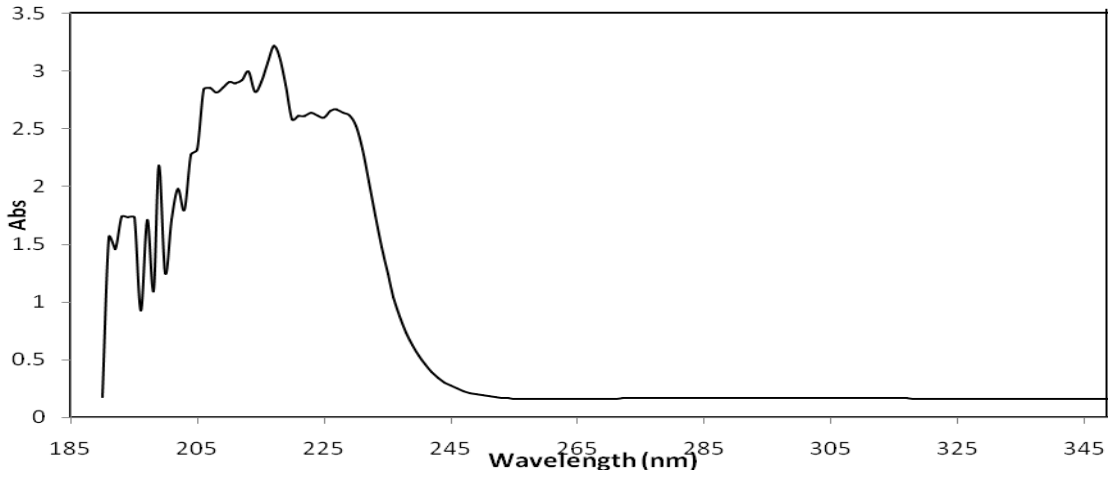

Figure 4: UV absorption spectrum for $NaNiO_2$ cathode material

3.5 Discharge Tests

The constructed half cells were discharged at different rates. This test was conducted mainly to find the charge initially retained in each of the cells corresponding to different discharging rates. 0.25, 0.5, 0.75, 1.0, 1.5 mA/g discharge rates were used to find the capacity in each of the cell.

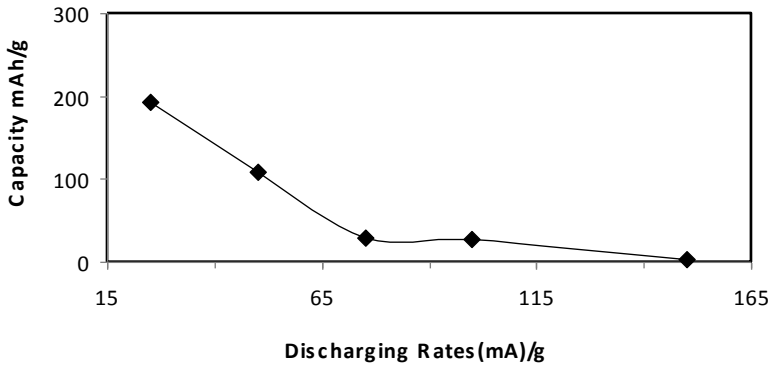

Figure 5: Discharging rates vs Retained capacity

Figure 5 illustrates the capacity per gram when discharged at different rates and the selective maximum retained charge. It can be monitored from the pattern that a maximum amount of charges retained corresponds to the 25 mA rate of charge per gram of active

material in cathode. After it reaching 75 mA per gram point the decline appears to be with a lower rate compared to the beginning as depicted in Figure 5.

3.6 Charge Discharge Analysis

The Sodium-Nickel half cell was charged by 7.5 mA g^{-1} for predetermined time periods where the corresponding discharging time was measured by discharging the cell with the rate of 0.75 mA g^{-1}. The distributive time spans of charging were selected as 150, 200, 300, 350, 450, 550 seconds by a rate of 7.5 mA g^{-1}. The discharging time corresponds to different rates of charging was used to calculate the retained capacity and thereby to construct charging time versus retained capacity trend line.

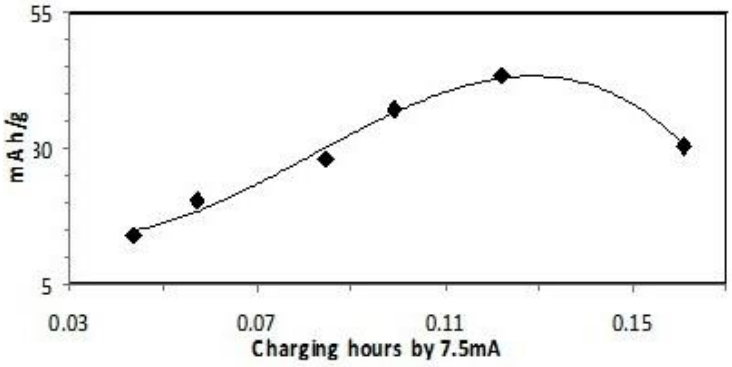

Figure 6: Charging vs Retained capacity

Figure 6 shows the charging hours by 7.5 mA g^{-1} versus capacity trend line and according to this graph a maximum rate of capacity is obtained by charging the cell by 7.5 mA g^{-1} for 0.12 hours. Also the graph highlights the fact that when the charging time exceeds this limit the retain capacity starts to decline dramatically.

3.7 Cyclic voltammetric Analysis

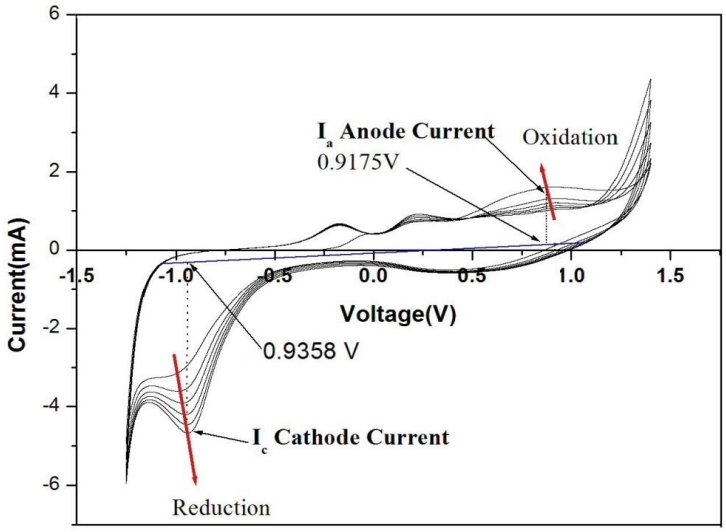

Figure 7: Cyclic voltammetric tests

The sample was scanned in the voltage range +1.45 V to -1.25 V at a rate of 0.1 Vs^{-1} to obtain the cyclic voltogram. As shown in the above diagram the oxidation peak was recorded at 0.9175 V and reduction peak incorporates at 0.9358 V. So the cell voltage can be calculated as a value of 1.8533 V which is almost same in the actual situation. Since the number of cycles in the figure has slight fluctuations which probably appears due to the irreversibility.

$$(+\text{ve})\text{Current} \quad Na^+ + e \rightarrow Na \qquad (1)$$
$$(-\text{Ve})\text{Current} \quad Na \rightarrow Na^+ + e \qquad (2)$$

3.8 Charge Discharge Tests.

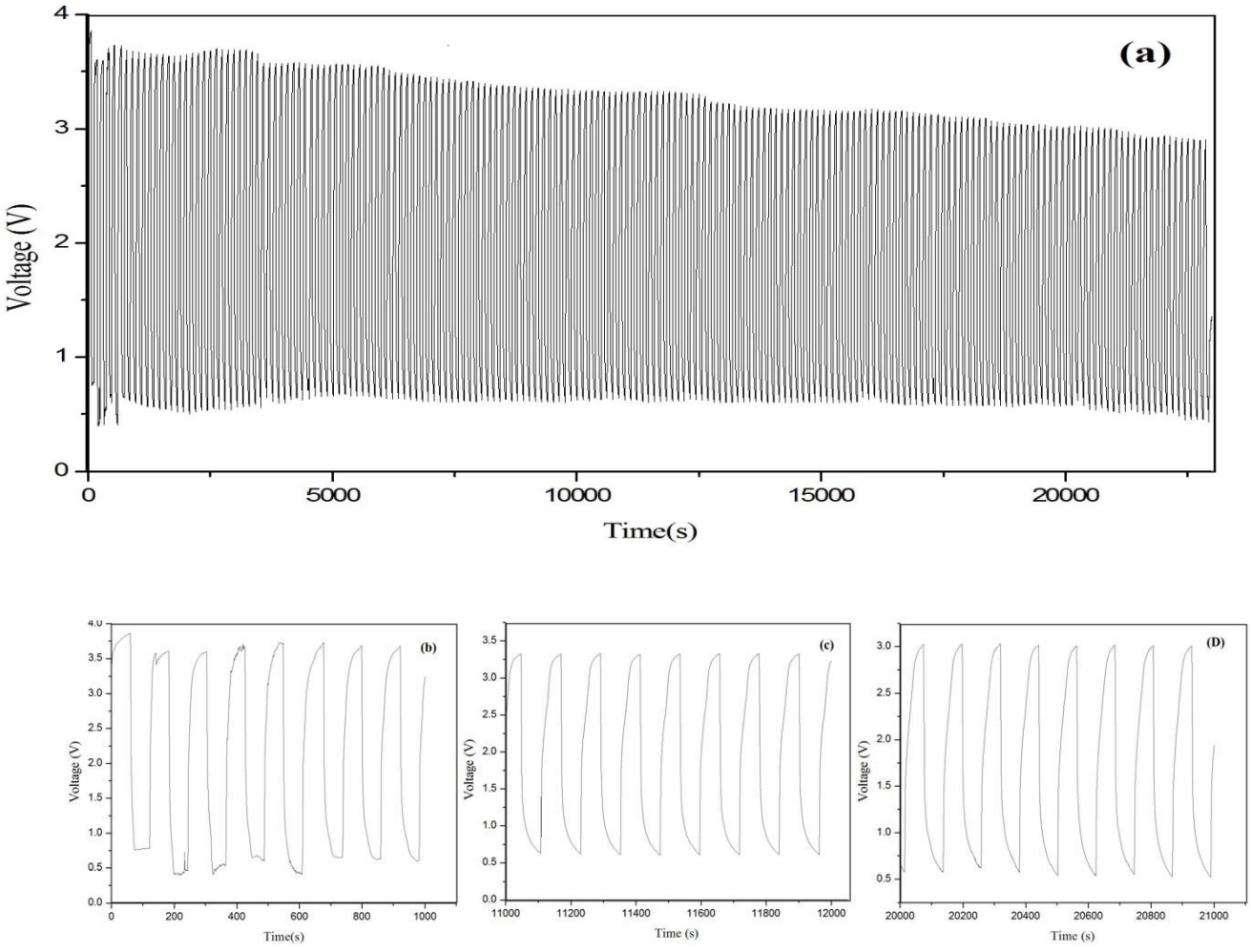

Figure 8: **(a)** Cycle Voltage vs Time – $NaNiO_2$, **(b)** Charge discharge cycles for first 1000 seconds, **(c)** Charge discharge cycles from 11,000 to 12,000 seconds, **(d)** Charge discharge cycles from 20,000 to 21,000 seconds

As shown in the Figure 8 the charge/discharge cyclability was tested for Sodium Nickel Oxide with 0.2 mA constant current for both charging and discharging. A voltage of 2.34 V was reported as the open voltage (no load) at the beginning and the half cell was kept for more than 180 charge-discharge cycles to perform including a rest time of one minute, for each of the cycle. At the end of 189th cycle, an average of a 2.8 V was recorded as the maximum at charged voltage which highlights the fact that after 189th charge/discharge cycle it still possesses the ability to hold the same amount of charges which could be retaining before. Nevertheless this was a positive indication of the retention of charges without a considerable draining. Both charge and discharge cycles were done with 0.2 A g^{-1}. The voltage was still maintaining at an average of above 0.46 V. Initial fluctuations in upper and lower levels of this drain tend to stabilize after 60th cycle. However, the battery seems to hold a fairly high reversibility level.

3.9 Impedance Tests

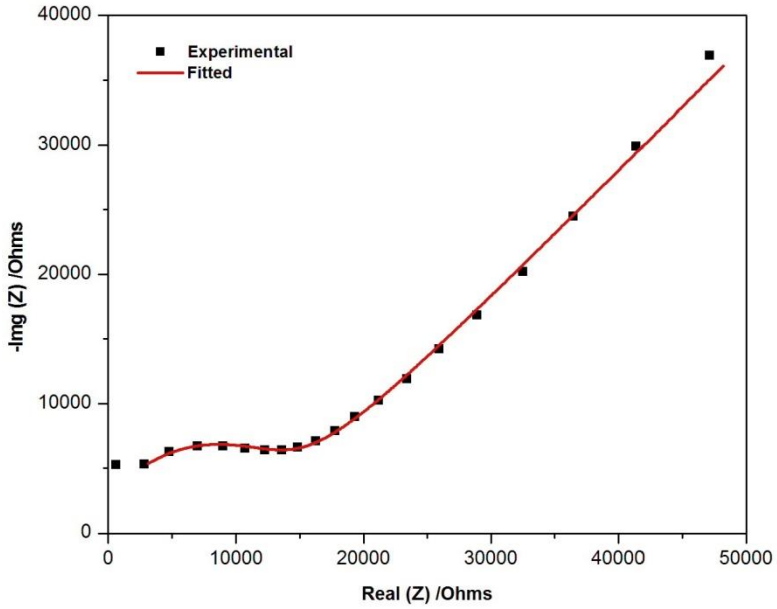

Figure 9: Nyquist plot for $NaNiO_2$ cell

The figure represents the Nyquist impedance plot for NaNi oxide cell. It was fitted with the possible fitting curve which is represented in solid line prior to the original curve represented in scattered data points. The equivalent circuit for the $NaNiO_2$ half cell is shown in Figure 10.

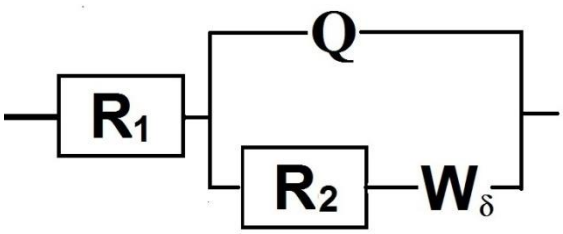

Figure 10: Equivalent circuit for the NaNi Oxide based, half-cell configuration Na metal (Anode) /PC-$NaClO_4$(electrolyte)/NaNiOxide (cathode material)

The value for R_1 = 332.8 Ω which represents combined effect of the metallic resistance of electrodes and resistance of the electrolyte. R_2 = 13121 Ω represented the charge transfer resistance of the cathode material. The Warburg impedance W_δ took the value to 356,886 Ω which represented the gravity of electrolyte of the NaNi oxide half cell. The double layer charge for the $NaNiO_2$ half cell was reported a value of $Q = 0.1131\times 10^{-9}$ $F.s^{(a-1)}$, where a = 0.9317.

4. CONCLUSION

The synthesis of Na_xNiO_2 nanoporous active material were made using solid state reactions at 700˚C and the prepared material was studied by XRD characterizing technique. The developed Na_xNiO_2 was used as the active cathode material in a Na-rechargeable cell. The characterization confirmed the crystal structure of $NaNiO_2$ to be the monoclinic structure, and morphology. Transition status test highlighted the specific energy band gap of 5.16 eV. Charge transfer resistance of the cathode material was 13,121 Ω. Elicit of maximum capacity retained relative for a gram of active material was possible with the fist discharges of each cell on varying discharging rates. It was revealed that a maximum rate of capacity is reported by charging the cell by 7.5 mA for 0.12 hours. The further increase in time beyond 0.12 hours responded with decrease in capacity. Since the structure depends on the magnetic parameters, magnetic studies are considered to be effective for determining the optimum synthesis conditions of $NaNiO_2$ cathode material. Therefore, the $NaNiO_2$ composite has been identified as an effective cathode material for sodium-ion batteries.

REFERENCES

1. F. Cheng et al., *Functional Materials for Rechargeable Batteries.* Advanced Materials, 23(15), (2011) 1695-1715.
2. J.M. Tarascon and M. Armand, *Issues and challenges facing rechargeable lithium batteries.* Nature, 414(6861), (2001) 359-367.

3. M. Armand and J.M. Tarascon, *Building better batteries.* Nature, 451(7179), (2008) 652-657.

4. B. Scrosati et al., *Recent advances in lithium ion battery materials.* Electrochimica Acta, 45(15–16), (2000) 2461-2466.

5. M.R. Palacin et al., *Recent advances in rechargeable battery materials: a chemist's perspective.* Chemical Society Reviews, 38(9), (2009) 2565-2575.

6. B. Dunn, H. Kamath and J.M. Tarascon, *Electrical Energy Storage for the Grid: A Battery of Choices.* Science, 334(6058), (2011) 928-935.

7. I. Terasaki and K. Uchinokura, *Large thermoelectric power in $NaCo_2O_4$ single crystals.* Phys. Rev. Lett. B, 56 **(**1997), R12685(R).

8. M.K. Aydinol and G. Ceder, *First-Principles Prediction of Insertion Potentials in Li-Mn Oxides for Secondary Li Batteries.* Journal of The Electrochemical Society, 144(11), (1997) 3832-3835.

9. N. Gayathri, S.K. Tiwary, R. Gundakaram, A. Anthony and C.N.R. Rao, *Electrical transport, magnetism, and magnetoresistance in ferromagnetic oxides with mixed exchange interactions.* Physical Review B condensed matter and materials physics, 56**, (**1997) 1345.

10. L.U.R. Benco et al., *First-principles prediction of voltages of lithiated oxides for lithium-ion batteries.* Solid State Ionics, 112(3–4), (1998) 255-259.

11. H. Ünlü et al., *A thermodynamic model for determining pressure and temperature effects on the bandgap energies and other properties of some semiconductors.* Solid-State Electronics, 35(9), (1992) 1343-1352.

12. J. Wang et al., *Analytical electrochemistry'*. VCH Inc., NY (1994).